

## Structure and oxygenase activity of the iron(II) complex with pyridylcarboxamide ligand

E. A. Turitsyna and A. A. Shteinman\*

*Institute of Problems of Chemical Physics, Russian Academy of Sciences,  
1 prosp. Akad. Semenova, 142432 Chernogolovka, Moscow Region, Russian Federation.  
Fax: +7 (496) 522 3507. E-mail: as237t@icp.ac.ru*

A reaction of  $\text{Fe}(\text{ClO}_4)_2 \cdot 6\text{H}_2\text{O}$  or  $\text{Fe}(\text{OTf})_2(\text{MeCN})_2$  with one equivalent of the tetradentate ligand bis(2-pyridyl)methyl-2-pyridylcarboxamide ( $\text{Py}_2\text{CHNHCOPy}$ , tpcaH) furnished dimeric iron(II) complexes  $[\text{Fe}(\text{tpcaH})_2]\text{X}_4$  ( $\text{X} = \text{ClO}_4^-$  (**1a**),  $\text{OTf}^-$  (**1b**)). According to the X-ray diffraction data for the complex **1a**, each iron atom is bound to the two pyridyl fragments of one ligand and the pyridylcarboxamide pair of the other one. Complex **1a** is a dimer in the crystalline state, while in MeCN solution according to the mass spectrometric data with the electrospray ionization,  $^1\text{H}$  NMR spectroscopic data, and quantum chemical calculations, it is apparently in the equilibrium with monomers of different structures. Complex **1** catalyzes selective oxidation of saturated hydrocarbons with hydrogen peroxide presumably involving the ferryl intermediate, which has an N,N,O-facial coordination of potentially tetradentate ligand tpcaH structurally modeling the 2-histidine-1-carboxylate-facial triad of the nonheme oxygenases.

**Key words:** NNO-oxygenase modeling, iron(II) complex with carboxamide, biomimetic oxidation.

Ability of some iron-containing enzymes to catalyze chemo-, regio-, and stereoselective oxidation of unactivated hydrocarbons stimulated a search for the corresponding biomimetic catalysts.<sup>1,2</sup> Together with the heme oxygenases, such as cytochrom P-450, attention of researches in the last years is attracted by the nonheme mononuclear and binuclear oxygenases, for example, the Riske dioxygenase<sup>3</sup> catalyzing dihydroxylation of a double bond and methane monooxygenase<sup>4</sup> selectively oxidizing methane under mild conditions.

Active centers of many mononuclear nonheme oxygenases have a common structural specificity: the presence of the so-called 2-histidine-1-carboxylate-facial triad<sup>3</sup> (Fig. 1), whose donor atoms (N, N, O) are in the coordination sphere of the iron atom in the mutual *cis*-arrangement with respect to each other, leaving the *trans*-coordination sites available for substrates and cofactors. During development of functional models for the nonheme oxygenases, it was found that dipyridyl and pyridylamine iron complexes containing two bidentate or one tetradentate ligand and having two labile *cis*-oriented coordination sites<sup>1,5</sup> (Fig. 2,  $\text{X} = \text{Py}$ ,  $\text{N}$ ) possess high catalytic activity. These catalysts assist in stereoselective hydroxylation of alkanes, epoxidation and *cis*-dihydroxylation of olefins using hydrogen peroxide as the oxidant. The high stereoselectivity of oxidation excluded participation of the  $\cdot\text{OH}$  radicals and chain radical processes and indicated involve-

ment of more selective ferryl intermediates<sup>5</sup>, such as  $\text{Fe}^{\text{IV}}=\text{O}$  or  $\text{Fe}^{\text{V}}=\text{O}$ , in the mechanism.

Though earlier models of the nonheme oxygenases contained only nitrogen donors, one should not forget that the coordination sphere of the iron atom of these oxygenases also includes, together with the nitrogen donors, one or more oxygen donors.<sup>3</sup> Studies on the effects of ligand surrounding of the iron atom in enzymes and their models on the catalytic activity is one of the most important directions in this field.<sup>1,4,5</sup> Coordination surrounding of the iron atom in the two representatives of mononuclear nonheme oxygenases, *viz.*, lipoxygenase and isopenicillinsynthase, contains a carboxamide ligand together with the

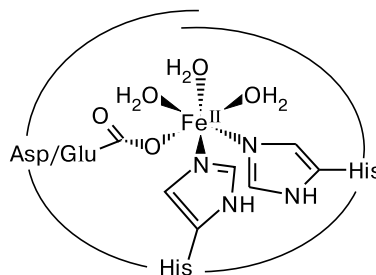


**Fig. 1.** The scheme of the active center of mononuclear nonheme oxygenases with 2-histidine-1-carboxylate-facial triad (the protein surrounding is arbitrary shown as a spiral circuit around the metal center).

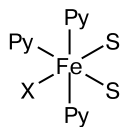


**Fig. 2.** The scheme of the iron atom coordination surrounding in dipyrityl  $[\text{Fe}_2\text{O}(\text{bipy})_4(\text{H}_2\text{O})_2]^{4+}$  ( $\text{X} = \text{Py}$ ), pyridylamine  $[\text{Fe}(\text{tpa})(\text{MeCN})_2]^{2+}$  ( $\text{X} = \text{N}$ ), and pyridylcarboxamide  $[\text{Fe}(\text{tpcaH})(\text{MeCN})_2]^{4+}$  (**1**) and  $[\text{Fe}(\text{tpcaH})(\text{MeCN})_2]^{2+}$  (**2**) ( $\text{X} = \text{NHCO}$ ) iron complexes, the functional models of the nonheme oxygenases; tpa is the  $(\text{PyCH}_2)_3\text{N}$ , tpcaH is the  $\text{Py}_2\text{CHNHCOPy}$ , S is the solvent.

N,N,O-facial triad.<sup>6</sup> These are the first examples of the amide ligation of the iron atom in oxygenases. Carboxamide ligand was also observed in other iron-containing peptides and proteins, such as the natural anticancer drug bleomycin and the enzyme nitrile hydratase.<sup>7,8</sup> Therefore, it is of interest to study effects of carboxamide donors on catalytic activity of chemical models of the mononuclear nonheme oxygenases. The structure and properties of iron complexes with some amide and amidate ligands were studied as the models of the active centers. The amidate donors stabilize higher oxidation states of metals similarly to the carboxylate donors.<sup>7</sup>

In the present work, we report on the structure and oxygenase activity of the  $\text{Fe}^{\text{II}}$  complex,  $[\text{Fe}(\text{tpcaH})(\text{MeCN})_2]^{4+}$  (**1**), with the tetradentate *N*-[bis-(2-pyridyl)methyl]-2-pyridylcarboxamide ligand (tpcaH) (see Fig. 2). Coordination chemistry of the tpcaH ligand has been studied earlier with the copper and iron atoms;<sup>9</sup> these complexes contained a deprotonated ligand in the meridional tridentate coordination. The carboxamide fragment is able to coordinate to the iron atom either by the amide nitrogen atom, or by the oxygen atom of the carbonyl group. In the first case, one can expect formation of the meridional complex mentioned above<sup>9</sup> or the complex  $[\text{Fe}(\text{tpcaH})(\text{MeCN})_2]^{2+}$  (**2**) (see Fig. 2), analogous to the complex  $[\text{Fe}(\text{tpa})(\text{MeCN})_2]^{2+}$  (tpa is the tripicolylamine) with two labile molecules of acetonitrile in the *cis*-position,<sup>5</sup> as it has been suggested by us earlier.<sup>10</sup> In the second case, the coordination surrounding of the iron atom is similar to the coordination surrounding of mononuclear nonheme oxygenases.<sup>3</sup> It has been recently found that an iron complex with the tridentate *N,N,O*-carboxamide ligand,  $[\text{Fe}^{\text{II}}(\text{Ph-dpaH})_2]^{2+}$  (Ph-dpaH is the di(2-pyridyl)-methylbenzamide) showed high catalytic activity in the stereospecific *cis*-dihydroxylation of olefins,<sup>11</sup> thus simulating such a function of the Riske NNO-dioxygenase.<sup>3</sup>

## Experimental

Reagents from Aldrich and Lancaster were used as purchased. Cyclohexane and *cis*-1,2-dimethylcyclohexane were filtered through the layer of silica gel before their use as substrates. Dichloromethane, acetonitrile, and *n*-hexane were distilled

under argon over  $\text{P}_2\text{O}_5$ ,  $\text{CaH}_2$ , and the sodium benzophenone ketyl, respectively. The iron salt  $\text{Fe}^{\text{II}}(\text{OTf})_2 \cdot 2\text{MeCN}$  (OTf is the trifluoromethanesulfonate) was obtained according to the published procedure.<sup>12</sup> The ligand tpcaH was obtained as described earlier.<sup>10</sup> Iron complexes were synthesized under argon in the Schlenk glassware, as well as in a glove box under nitrogen. Elemental analysis was performed in the Microanalytical Laboratory of IPChPh RAS.

Electron absorption spectra were recorded on Specord M-40 or Varian 300 Bio UV/vis spectrophotometers. IR spectra were recorded on Specord 75-IR and Specord M-82 spectrometers. Mass spectrometric measurements with the electrospray ionization (ESI) (acetonitrile) were performed on a high resolution time-of-flight mass spectrometer in the Institute of Energy Problems of Chemical Physics of RAS.<sup>13</sup>  $^1\text{H}$  NMR spectra in acetonitrile- $d_3$  were recorded on a Varian UNITY spectrometer (300 MHz), chemical shifts are given in the  $\delta$  scale relatively to the signal of the solvent residual protons. NQR spectra were recorded on a standard spectrometer with the source of  $^{57}\text{Co}(\text{Rh})$  at the temperature of liquid nitrogen, the isomeric shifts were referenced to the metallic iron.

X-ray diffraction analysis for the complex **1** was performed in the Laboratory of Crystallography, Department of Chemistry, University of Minnesota. A crystal (of approximate size  $0.20 \times 0.10 \times 0.10$  mm) was placed on a glass capillary tip 0.1 mm in diameter on a Siemens SMART Platform CCD diffractometer for collection of the data at 173(2) K using Mo- $\text{K}\alpha$  radiation (graphite monochromator). The structure was solved using the SIR97 program and refined using the SHELXR-97 program. All the nonhydrogen atoms were set geometrically and refined in the anisotropic full-matrix approximation on  $F^2$ , whereas all the hydrogen atoms were placed in the ideal positions and refined in the isotropic approximation.

Quantum chemical calculations were performed using the Gaussian-03 program. Optimization of different spin states for iron complexes was performed using the B3LYP/LanL2DZ approximation with the associated ECP for iron. Optimization of geometric structures of the high-spin complexes was performed on the B3LYP theory level using the 6-31G\*\* basis set. The accurate calculations for the energy were performed using the SDD basis set with the associated ECP for iron and the 6-311G\*\* basis set for other atoms. The free energies in acetonitrile were calculated at 298 K using the SCRF method in the framework of the polarizing continuum model (PCM) and include the accurate values of energy calculated at B3LYP/6-31G\*\* & SDD//B3LYP/LanL2DZ, as well as the zero (ZPE) and thermal corrections and corrections on solvation calculated on the B3LYP/LanL2DZ theory level.

The following procedure was used for the study of the oxidation reaction. A calculated amount of 35% aqueous  $\text{H}_2\text{O}_2$  was added in one portion to a solution of **1** in acetonitrile with the concentration  $1 \text{ mmol L}^{-1}$  (2 mL) containing a 1000-fold excess of hydrocarbon (RH) with vigorous stirring at room temperature in air in such a way that the concentration of  $\text{H}_2\text{O}_2$  in the reaction solution exceeded the concentration of complex **1** by 400 times, and this moment was considered as a beginning of the time counting. Then the stirring was continued less vigorously collecting samples for analysis through the certain periods of time. The oxidation products were analyzed on a Hewlett—Packard 5880A chromatograph with the flame-ionizing detector and a Carbowax 20M capillary column.

**[Fe<sup>II</sup><sub>2</sub>(tpcaH)<sub>2</sub>(MeCN)<sub>4</sub>](ClO<sub>4</sub>)<sub>4</sub> (**1a**).** (Attention! The perchlorate salts are potential explosives and should be handled with precautions). A solution of Fe<sup>II</sup>(ClO<sub>4</sub>)<sub>2</sub> · 6H<sub>2</sub>O (0.36 g, 1.0 mmol) in MeCN (5 mL) was added to a stirred solution of the ligand tpcaH (0.29 g, 1 mmol) in MeCN (5 mL). A clear light orange solution that obtained was stirred for 30 min at room temperature, followed by addition of the equal volume of diethyl ether. The solution was kept at –25 °C for 16 h to obtain orange crystals of complex **1a** (0.5 g, 80%). Diffusion of the diethyl ether vapors into the saturated solution of complex **1a** in MeCN over 3 days gave cubic crystals of **1a** suitable for X-ray diffraction studies. UV (MeCN), λ<sub>max</sub>/nm (ε/L mol<sup>–1</sup> cm<sup>–1</sup>): 265 (8600), 356 (1500), 425 (650), 460 (370), 850 (30). IR (KBr), ν/cm<sup>–1</sup>: 1635, 1601, 1534, 1470, 1440, 1376, 1162, 1049, 1012, 760. <sup>1</sup>H NMR (CD<sub>3</sub>CN, 25 °C), δ: 39.1, 49.4, 60.3, 63.5, 68.3, 82.9, 86.9, 95.6. <sup>1</sup>H NMR ((CD<sub>3</sub>)<sub>2</sub>CO, 25 °C), δ: 22.8, 43.8, 58.0, 71.0, 107.0. NQR, mm s<sup>–1</sup>: δ = 1.18, ΔE<sub>Q</sub> = 2.05. MS (ESI), *m/z* (*I*<sub>rel</sub> (%)): 193.4 [1/2 M – MeCN]<sup>2+</sup> (25), 213.74 [1/2 M]<sup>2+</sup> (100), 444.79 [1/2 M – 2 MeCN + ClO<sub>4</sub>]<sup>+</sup> (63), 634.06 (20), 734.78 (18). Found (%): C, 39.85; H, 3.10; N, 13.23; Cl, 11.50. C<sub>21</sub>H<sub>20</sub>N<sub>6</sub>O<sub>9</sub>Cl<sub>2</sub>Fe. Calculated (%): C, 40.21; H, 3.21; N, 13.40; Cl, 11.31.

**Complex [Fe<sup>II</sup><sub>2</sub>(tpcaH)<sub>2</sub>(MeCN)<sub>4</sub>](OTf)<sub>4</sub> (**1b**).** A mixture of the equimolar amounts of Fe<sup>II</sup>(OTf)<sub>2</sub> · 2MeCN and tpcaH in the CH<sub>2</sub>Cl<sub>2</sub>–MeCN (10 : 1) solvent mixture was stirred for 30 min and filtered, hexane was poured on top of the clear solution that obtained. The mixture was kept at –25 °C for 16 h to obtain orange crystals of **1b** in 89% yield. UV (MeCN), λ<sub>max</sub>/nm (ε/L mol<sup>–1</sup> cm<sup>–1</sup>): 262 (9000), 354 (1500), 425 (700), 478 (350), 870 (50). IR (KBr), ν/cm<sup>–1</sup>: 1639, 1595, 1560, 1482, 1445, 1385, 1246, 1170, 1031, 761, 638, 517. <sup>1</sup>H NMR ((CD<sub>3</sub>)<sub>2</sub>CO, 25 °C), δ: –82, 26.0, 42.8, 56.9, 67.0, 105.2, 123.9. MS (ESI), *m/z* (*I*<sub>rel</sub> (%)): 193.41 [1/2 M – MeCN]<sup>2+</sup> (65), 213.74 [1/2 M]<sup>2+</sup> (100), 494.41 [1/2 M – 2 MeCN + CF<sub>3</sub>SO<sub>3</sub>]<sup>+</sup> (30).

## Results and Discussion

Iron(II) complexes with the tetradentate ligand tpcaH were synthesized with both the perchlorate (**1a**) and triflate (**1b**) counterions by mixing the equimolar solutions of the corresponding iron salts and the tpcaH ligand with subsequent precipitation of crystals. The media for the reactions (solvents for precipitation) were as follows: MeCN (Et<sub>2</sub>O) for the perchlorate **1a** and CH<sub>2</sub>Cl<sub>2</sub>–MeCN, 10 : 1, (hexane) for the triflate **1b**. According to the microanalytical data, the complex **1a** contains one ligand per iron atom.

The IR spectrum of the free ligand exhibits bands characteristic of the carboxamide group: a sharp and strong band at 3350 cm<sup>–1</sup> (ν<sub>NH</sub>) and strong bands at 1670 cm<sup>–1</sup> (ν<sub>CO</sub>, the "amide band I") and 1504 cm<sup>–1</sup> (δ<sub>NH</sub>, the "amide band II").<sup>14</sup> Formation of complex **1** leads to the weakening and broadening the band at 3350 cm<sup>–1</sup> whereas the amide band I is shifted toward lower frequencies (Δν = 35 cm<sup>–1</sup>). This indicates the fact that in the crystalline state of the complex **1**, the carboxamide tpcaH ligand is coordinated to the iron atom with the oxygen atom of the carbonyl group, rather than with the nitrogen atom of the carbamide group.<sup>15</sup> The bands at ~1600 cm<sup>–1</sup> are related to the deformations characteristic of the pyridine

ring. According to the EAS, <sup>1</sup>H NMR and Mossbauer spectroscopy, the complex **1** contains the iron(II) atom in the high-spin state. Thus, the electron spectrum of **1a** exhibits two strong bands at 356 and 425 nm and weaker bands at 460 and 850 nm. The weak low-energy band can be assigned to the transition <sup>5</sup>T<sub>2g</sub> → <sup>5</sup>E<sub>g</sub>, the only spin-allowed transition for the d<sup>6</sup> high-spin octahedral state of the Fe<sup>II</sup> ion.<sup>8</sup> The high-energy bands are also characteristic of the bands for the d<sup>6</sup> high-spin state of the Fe<sup>II</sup> ion. Note that the presence of the wide region of narrow signals in the <sup>1</sup>H NMR spectrum agrees with the high-spin nature of the complex **1**. A complex structure of the <sup>1</sup>H NMR spectrum does not allow us to reliably assign signals of the proton resonance, but indicates the presence of several individual compounds in the solution of complex **1** in acetonitrile. Finally, the NQR spectrum of the complex **1a** exhibits an isomeric shift and a quadrupole splitting typical of the high-spin iron(II) ion in the N/O-coordination surrounding.

The crystal structure of complex **1**, studied for the complex **1a** as an example (Fig. 3, Tables 1 and 2), contrary to our initial expectation,<sup>10</sup> differs from the structure of the complex [Fe(tpa)(MeCN)<sub>2</sub>](ClO<sub>4</sub>)<sub>2</sub> and is a centrosymmetric dimer. As it is seen from Fig. 3, this structure has two iron atoms bound with two tpcaH bridges. Each Fe<sup>II</sup> center in the complex **1a** is in the distorted octahedral surrounding (see Table 2) containing two adjacent pyridyl fragments (N(23)–Fe(1)–N(24) and N(3)–Fe(2)–N(4)) of one ligand and a pyridylcarboxamide fragment (N(2)–Fe(1)–O(20) and N(22)–Fe(2)–O(21)) of another ligand, as well as two coordinated molecules of acetonitrile. In this dimer, the pyridyl-2-carboxamide fragment of the ligand is coordinated to the Fe<sup>II</sup> center with the carbonyl oxygen atom and the pyridyl fragment as a bidentate chelating ligand, which is confirmed by the IR spectroscopic data. This type of coordination of pyridyl-2-carboxamide fragment is not unusual and has been observed earlier<sup>16</sup> in some Cu<sup>II</sup> complexes. The principal bond distances and bond angles of the complex **1a** are given in Table 2. An average distance for the Fe–N<sub>py</sub> bond is 2.20 Å and comparable with the typical values for the high-spin iron(II) complexes, such as complexes with the 6-Me<sub>3</sub>tpa ligand.<sup>17</sup> The tpcaH ligand containing undissociated amide is able to act as a tetradentate ligand, in contrast to the tpca<sup>–</sup> anion, which coordinates the iron(II) and iron(III) ions, as well as the copper(II) ion as a tridentate ligand.

The <sup>1</sup>H NMR spectra and mass spectra indicate that the complex **1**, being a dimer in the crystalline state, does not preserve its structure in solutions and apparently dissociates to the monomeric state. Taking into account that two isomers are possible for the monomeric particles with coordination of carboxamide by the nitrogen atom or the oxygen atom, at least three iron complexes can be present in solution: a dimeric form (D) and two monomeric forms (M<sub>1</sub> and M<sub>2</sub>). Since the experimental data do not allow us

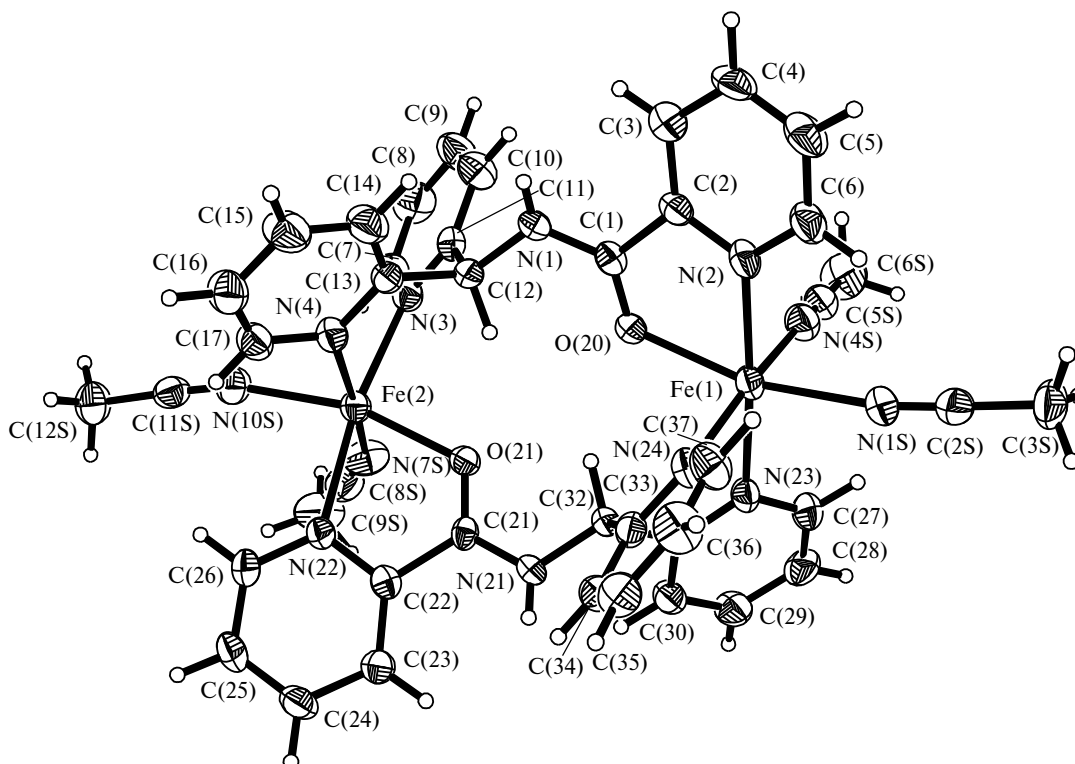


Fig. 3. The structure of cation in the complex **1a** according to the X-ray crystallographic data.

to determine relative concentrations of these particles in solution, we undertook calculations of relative stabilities

**Table 1.** Crystallographic data and parameters of the X-ray diffraction experiment for the complex **1a**

Parameter	Value
Molecular formula	$C_{42}H_{40}N_{12}O_{18}Cl_4Fe_2$
Molecular weight	1254.360
Crystal system	Triclinic
Space group	$P\bar{1}$
Cell sizes	
$a/\text{\AA}$	12.080(2)
$b/\text{\AA}$	15.837(2)
$c/\text{\AA}$	16.944(3)
$\alpha/\text{deg}$	91.233(3)
$\beta/\text{deg}$	100.531(3)
$\gamma/\text{deg}$	104.669(3)
$V/\text{\AA}^3$	3075.3(8)
$Z$	2
$d_{\text{calc}}/\text{g cm}^{-3}$	1.532
$\mu/\text{cm}^{-1}$	0.0728
Region of scanning, $\theta/\text{deg}$	1.33–25.08
All reflections	18386
Number of independent reflections	10752
$R_{\text{int}}$	0.041
Number of observed reflections	7213
GOF on $F^2$	1.022
$R$ -factors on $I > 2\sigma(I)$	
$R_1$	0.0509
$wR_2$	0.120

of the complexes for solutions in acetonitrile in the framework of electron density functional theory (DFT) in order to evaluate their concentrations. The DFT is a reliable and acceptable instrument for calculations of geometry and energy parameters of iron complexes<sup>18</sup> and allows one to evaluate relative stabilities of suggested complexes in solution. To check reliability of the chosen approximations, we initially calculated geometry and energy of various multiplet states for the starting complex **1**. The results given in Table 3 show that the calculations predict for this

**Table 2.** Principal bond distances ( $d$ ) and bond angles ( $\omega$ ) in the structure of **1a**

Bond	$d/\text{\AA}$	Angle	$\omega/\text{deg}$
Fe(1)—O(20)	2.131(3)	O(20)—Fe(1)—N(1S)	165.05(12)
Fe(1)—N(2)	2.208(3)	O(20)—Fe(1)—N(24)	90.12(11)
Fe(1)—N(23)	2.188(3)	O(20)—Fe(1)—N(4S)	89.59(12)
Fe(1)—N(24)	2.179(3)	O(20)—Fe(1)—N(23)	100.70(11)
Fe(1)—N(1S)	2.168(4)	O(20)—Fe(1)—N(2)	74.60(11)
Fe(1)—N(4S)	2.182(4)	N(1S)—Fe(1)—N(24)	95.80(13)
Fe(1)—Fe(2)	6.796(13)	N(1S)—Fe(1)—N(4S)	87.18(14)
Fe(2)—O(21)	2.113(3)	N(1S)—Fe(1)—N(23)	93.66(13)
Fe(2)—N(3)	2.182(3)	N(1S)—Fe(1)—N(2)	90.97(12)
Fe(2)—N(4)	2.163(3)	N(24)—Fe(1)—N(4S)	169.01(13)
Fe(2)—N(22)	2.251(3)	N(24)—Fe(1)—N(23)	82.96(12)
Fe(2)—N(7S)	2.136(4)	N(24)—Fe(1)—N(2)	97.83(12)
Fe(2)—N(10S)	2.160(4)	N(4S)—Fe(1)—N(23)	86.30(12)
		N(4S)—Fe(1)—N(2)	92.68(13)
		N(23)—Fe(1)—N(2)	175.20(12)

**Table 3.** Comparison of the X-ray diffraction data for complex **1** with the DFT quantum chemical calculations for the spin states (s)

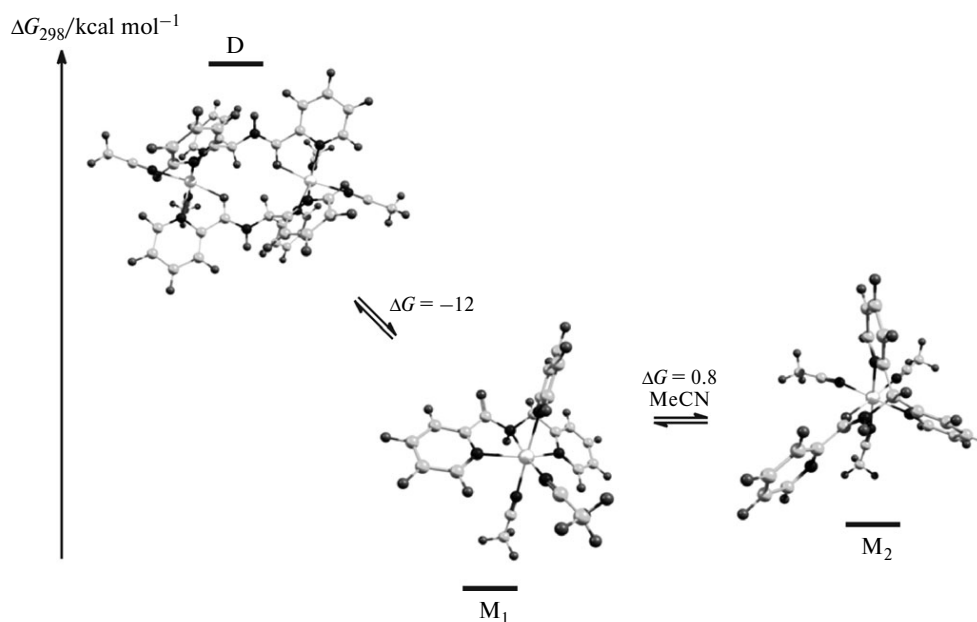
Parameter of comparison	X-ray data	Calculations		
		s = 2	s = 1	s = 0
$d(\text{Fe}—\text{Fe})/\text{\AA}$	6.7962(13)	6.904	7.038	7.125
$d((\text{Fe}—\text{O})_{\text{cp}})/\text{\AA}$	2.122(3)	2.165	2.152	2.287
$d((\text{Fe}—\text{N})_{\text{cp}})/\text{\AA}$	2.182(4)	2.233	2.115	2.066
$\Delta E/\text{kcal mol}^{-1}$		0	22.7	13.1

complex a high-spin ground state with four unpaired electrons on each iron atom, which agrees with the experimental data. The average bond distances between the iron atom and its closest coordination surrounding calculated for this state satisfactorily agree with the values found by X-ray diffraction studies. Figure 4 shows the calculation results for  $\Delta G_{298}$  for the high-spin states of suggested complexes in solution of acetonitrile based on the most simple polarizing continuum model (PCM). According to these calculations, the suggested monomeric complexes have also a high-spin ground state. It is seen that the starting dimeric complex is unstable with respect to decomposition to monomers, whereas two isomeric monomers possess virtually the same stability with respect to each other. However, involvement of acetonitrile molecule shifts the equilibrium to the side of monomeric form  $M_2$ . To sum up, the monomeric complexes should predominate in solution of acetonitrile over the dimer, and the monomer  $M_2$  is apparently the major one, though not obligatory deter-

mining the catalytic activity in solution. However, it can be suggested that the exchange of the relatively strong donor, pyridine, with a weaker one, acetonitrile, makes the complex  $M_2$  more electron-accepting and, consequently, its ferryl intermediate should be more reactive than  $M_1$ . Proceeding from these assumptions and taking into account the higher concentration of complex  $M_2$ , one can conclude that this complex will apparently determine the catalytic activity of complex **1** in solutions. This conclusion agrees with the high activity of such FeNNO-centers observed in oxygenases and their models.<sup>3</sup>

The complex **1** was studied as a catalyst for the oxidation of alkanes using hydrogen peroxide as a terminal oxidant. Alcohols and ketones were the only products (Table 4) with the total number of the catalytic cycles (TON) equal to 50 over 53 h in the case of cyclohexane, which indicates "vitality" of the complex under the reaction conditions. During carrying out these experiments, it was noted that the ratio of the concentrations of alcohol and ketone  $[A]/[K]$  smoothly changes in the course of the reaction, which apparently indicates the changing degree of involvement in the process of two or more active intermediates with different selectivity. The extent of retention of configuration (RC) on hydroxylation of the tertiary C—H bond in *cis*-1,2-dimethylcyclohexane was also lower at the beginning of the reaction.

Though the high chemo- and stereoselectivity in the catalytic oxidation involving complex **1** undoubtedly indicates the fact that the metal-oxygen intermediate is the active oxidant in this biomimetic system,<sup>19</sup> attempts to detect this active intermediate using ESI mass spectrometry have proved unsuccessful. Apparently, this ferryl inter-

**Fig. 4.** Thermodynamics of the iron(II) complex ions with the carboxamide tpcaH ligand in MeCN according to the DFT calculations in the framework of the polarizing continuum model.

**Table 4.** Oxidation of cyclohexane and *cis*-1,2-dimethylcyclohexane (DMCH) with hydrogen peroxide catalyzed by the complex **1**\*

Reaction time/h	Cyclohexane				DMCH RC (%)
	Cyclohexanol, TON	Cyclohexanone, TON	[A]/[K]	Conversion of H <sub>2</sub> O <sub>2</sub> (%)	
0.5	7.8	2.7	2.9	3.3	87
1.0	14.2	2.8	5.1	4.1	92
2.0	18.2	3.0	6.1	6.0	98
2.5	21.8	3.2	6.8	7.0	97
4.0	24.3	3.5	6.9	7.8	97
5.0	27.5	4.6	6.0	9.2	96

*Note.* [A]/[K] is the ratio of concentrations of the alcohol (A) and ketone (K) formed in the oxidation of cyclohexane. RC is the degree of retention of configuration in the oxidation of the tertiary C—H bond in *cis*-1,2-dimethylcyclohexane (DMCH),  $RC = 100\% (cis\text{-ol} - trans\text{-ol}) / (cis\text{-ol} + trans\text{-ol})$ , where *cis*-ol and *trans*-ol are the concentrations of the formed alcohol with *cis*- and *trans*-configurations, respectively.

\* Reaction conditions:  $C_1 = 1 \text{ mmol L}^{-1}$ , **1** : H<sub>2</sub>O<sub>2</sub> : RH = 1 : 400 : 1000, 20 °C.

mediate has a mononuclear nature. According to the DFT calculations, Fe(tpca)(MeCN)<sub>3</sub> is the major mononuclear complex in the catalytic solution, whose ligand uses the tridentate facial N,N,O-donor set for the coordination with the iron atom. Such a coordination is structurally similar to the 2-histidine-1-carboxylate-(N,N,O)-facial coordination in the mononuclear nonheme oxygenases (see Fig. 1). The peroxide intermediate Fe<sup>III</sup>—OOH is the first metal-oxygen intermediate in the reaction of H<sub>2</sub>O<sub>2</sub> with such a center in enzymes or their models.<sup>20</sup> A possibility of formation of such an intermediate upon catalysis with complex **1** is confirmed by the spectral observation of the formation of the alkylperoxide intermediate with  $\lambda_{\text{max}} = 578 \text{ nm}$  at  $-40^\circ\text{C}$  upon treatment of the solution of complex **1** with five equivalents of Bu<sup>t</sup>OOH in MeCN. The effective rate constant of decomposition of this intermediate  $k_d = 0.0015 \text{ s}^{-1}$  ( $-40^\circ\text{C}$ ) is close to that found<sup>21</sup> for the complexes [(tpa)Fe<sup>III</sup>OOH]<sup>2+</sup> ( $k_d = 0.002 \text{ s}^{-1}$  ( $-45^\circ\text{C}$ )) and [(tpa)Fe<sup>III</sup>OObu<sup>t</sup>]<sup>2+</sup> ( $k_d = 0.0015 \text{ s}^{-1}$  ( $-30^\circ\text{C}$ )). The heterolytic cleavage of the O—O bond in the peroxide intermediate should lead to the formation of the intermediate (MeCN)<sub>n</sub>(tpcaH)Fe<sup>V</sup>=O, which apparently oxygenates alkanes by the transfer of the O atom on them *via* the oxygen rebound mechanism.<sup>22</sup>

In conclusion, the iron(II) complex with carboxamide ligand (1 : 1) is a dimer in the crystalline state, whereas in solution according to the mass spectrometric (ESI) and <sup>1</sup>H NMR spectroscopic data and quantum chemical calculations, it is apparently present in the equilibrium with a monomeric form. The monomeric form predominantly

existing in solution contains the N,N,O-facial triad and the iron(II) atom in the high-spin state and, consequently, structurally simulates an active center of the mononuclear nonheme oxygenases (see Fig. 1). The complex **1** has proved an efficient biomimetic catalyst capable to oxygenate alkanes with high selectivity. In the oxidation of alkanes, this complex showed high stability (in the presence of aggressive oxidative medium) allowing one to reach up to 50 catalytic cycles in the oxidation of cyclohexane.<sup>10</sup>

The authors are grateful to W. W. Brennessel and V. G. Young, Jr. (the Laboratory of Crystallography, Department of Chemistry of University of Minnesota) for carrying out the X-ray studies for complex **1a** and prof. L. Que, Jr. (University of Minnesota) for providing a work-place for A. A. Shteinman in his laboratory.

## References

1. A. A. Shteinman, *Usp. Khim.*, 2008, **77**, 1013 [*Russ. Chem. Rev. (Engl. Transl.)*, 2008, **77**, 945].
2. L. Que, Jr., W. B. Tolman, *Nature*, 2008, **455**, 333.
3. K. D. Koehn, J. P. Emerson, L. Que, Jr., *J. Biol. Inorg. Chem.*, 2005, **10**, 87.
4. E. Y. Tshuva, S. J. Lippard, *Chem. Rev.*, 2004, **104**, 987.
5. P. D. Oldenburg, L. Que, Jr., *J. Mol. Catal. A*, 2006, **117**, 15.
6. E. L. Hegg, L. Que, Jr., *Eur. J. Biochem.*, 1997, **250**, 625.
7. D. N. Marlin, P. K. Masharak, *Chem. Soc. Rev.*, 2000, **29**, 69.
8. E. I. Solomon, T. C. Brunold, M. I. Davis, J. N. Kemsley, S.-K. Lee, N. Lehnert, F. Neese, A. J. Skulan, Y.-S. Yang, J. Zhou, *Chem. Rev.*, 2000, **100**, 235.
9. S. Zhu, W. W. Brennessel, R. G. Harrison, L. Que, Jr., *Inorg. Chim. Acta*, 2002, **337**, 32.
10. E. A. Gutkina, T. B. Rubtsova, A. A. Shteinman, *Kinet. i Katal.*, 2003, **44**, 116 [*Kinet. Catal. (Engl. Transl.)*, 2003, **44**, 106].
11. P. D. Oldenburg, A. A. Shteinman, L. Que, Jr., *J. Am. Chem. Soc.*, 2005, **127**, 15672.
12. K. S. Hagen, *Inorg. Chem.*, 2000, **39**, 5867.
13. O. A. Mirgorodskaja, A. A. Shevchenko, A. F. Dodonov, *Anal. Chem.*, 1994, **66**, 99.
14. R. L. Chapmen, K. C. Vagg, *Inorg. Chim. Acta*, 1979, **33**, 227.
15. P. Maslak, J. J. Szczepanski, M. Parves, *J. Am. Chem. Soc.*, 1991, **113**, 1062.
16. Y. Kajikawa, N. Azuma, K. Tajima, *Inorg. Chim. Acta*, 1998, **283**, 61.
17. Y. Zang, J. Kim, Y. Dong, E. C. Wilkinson, E. H. Appelman, L. Que, Jr., *J. Am. Chem. Soc.*, 1997, **119**, 4197.
18. P. E. M. Siegbahn, F. Himo, *J. Biol. Inorg. Chem.*, 2009, **14**, 643.
19. V. S. Kulikova, O. N. Gritsenko, A. A. Shteinman, *Mendeleev Commun.*, 1996, **6**, 119.
20. K. Chen, L. Que, Jr., *J. Am. Chem. Soc.*, 2001, **123**, 6327.
21. J.-J. Girerd, F. Banse, A. J. Simaan, *Struct. Bonding*, 2000, **97**, 145.
22. J. T. Groves, *J. Inorg. Biochem.*, 2006, **100**, 434.

Received February 22, 2011;  
in revised form August 24, 2011